International Journal of Heat and Technology
Vol. 40, No. 6, December, 2022, pp. 1424-1431
Journal homepage: http://iieta.org/journals/ijht

The Numerical Simulation of Thermal Efficiency of Triple Pipe Heat Exchanger Using PCMs (Paraffin and Lauric Acid) System

Haider Hakeem Kareem*, Fawziea M. Hussien, Johain J. Faraj

Middle Technical University Engineering Technical College-Baghdad, Baghdad 10074, Iraq

Corresponding Author Email: haiderhakeem42@gmail.com

https://doi.org/10.18280/ijht.400609

Received: 28 November 2022
Accepted: 20 December 2022

Keywords:
triple pipe heat exchanger, lauric acid, paraffin, PCM

ABSTRACT

COMSOL Multiphysics is used to adequately study the numerical modeling of phase change material behavior in a triple heat exchanger. The triple heat exchanger comprises three sides: an interior pipe for water cooling and heating, an annular space between the second and first interior pipes conveying Paraffin, and a third side annular space between the outer pipe and the second pipe holding Lauric acid. The dimensions of the triple heat exchanger are as follows: 30 cm length and side diameters of (0.5 in: 2.5 in: 3.5 in). Overall, the patterns reveal that the CFD and experimental work are in perfect agreement. PCM 2 is more reliable than paraffin. As the flow rate rises, the validity decreases; the maximum validation is obtained at 11 L/min. The results shows that the number of fins enhances efficiency by 5% (from 6 to 4); any number of fins over 6 promotes no more efficiency percentage. The additional fins are considered to produce increased heat transfer resistance, resulting in a significant increase in heat transmission. Copper slightly conducts heat better than aluminum and iron. Aluminum is the best material; its efficiency is equivalent to copper's. The diameter of the pipe has no effect on the percentage of paraffin efficiency. The better the heat resistance with an uniform heat transfer area between the paraffin and lauric acid layers, the broader the diameter of the lauric acid layer. Improving the outer diameter of the heat charge process implies increasing the efficiency percentage. The highest efficiency% is seen at 4.5 in.

1. INTRODUCTION

Energy conservation is a popular issue nowadays. Increasing energy demand and diminishing fossil resources necessitate alternative energy sources. Nature delivers plentiful, free, pollution-free, readily used, continuous solar energy. This thermal energy is stored as latent, sensible, and thermo-chemical energy (TCES). In latent thermal energy storage, a solid-to-liquid or liquid-to-solid phase shift occurs while the system's temperature remains unchanged. In STESs, only material temperature raises to store heat. High-temperature STESs need chemical stability and heat capacity. In thermo-chemical energy storage (TCES) devices, chemical processes store and recover thermal energy. TCES need regulated settings and have limited lifespans. Latent thermal energy storage (LT- ESS) systems based on phase change material (PCM) may store substantial amounts of heat at low operating temperatures [1]. PCMs store sensible and latent heat for heating and cooling. Low temperature energy storage systems are used in solar air collectors [2], heating and cooling systems for electronics [3], thermal storage of building structures and refrigeration [4], drying technology, building equipment such as domestic hot water [5], cold storage, and waste heat recovery systems. Gas phase change systems are not practicable due to massive volumetric changes, but in solid-solid phase transition, PCMs' crystalline structure changes, resulting in thermal energy storage, although at a sluggish pace and poor energy storage density [6]. Because of their modest volumetric change, ease of handling, high thermal energy density, and compactness, PCMS with solid-liquid transition dominate [7]. Most known materials display solid-liquid transition, however common applications need the following qualities [8, 9].

Paraffin (waxes) are n-alkane mixes, Cn $H(2n^{+2})$. They're refinery byproducts. Paraffin phase transition temperatures are 18 to 71°C [10], hence it may be utilized at low temperatures. Large-scale, low-cost manufacturing compared to pure n-alkanes. Chemical stability, low vapor pressure, no phase separation, self-nucleation, and high latent heat density are desirable qualities of paraffins. However, their mild flammability, poor container compatibility, fluidity, and low thermal conductivity make their employment difficult [11]. Using heat transfer augmentation strategies may fix poor thermal conductivity. Heat transfer fins, multi-tubes, Nano-particles in PCMs, and shell shape changes. These strategies may be examined experimentally and numerically (theoretically). Carboxylic acids with chemical formula CH_3 $(CH_2)2n$ COOH and long chain hydrocarbons are called as fatty acids. As an advantage eutectic mixture can be formed by mixing two or more fatty acids. Their phase transition temperature ranges from 16 to 74°C [12].

PCM melting is dominated by natural convection. The buoyancy forces improve heat transmission by generating flow vortices. Orientation of heat surface affects natural convection and PCM melting time (tm). PCMs' limited thermal conductivity makes heat transmission challenging. PCM-based thermal energy storage devices must enhance heat transmission. As a cure for shell-and-tube LTESS's poor

thermal performance, several HTF tubes are used in the PCM to improve heat transmission. Agyenim et al. [13] employed erythritol as a PCM to test the thermal energy storage capability of a horizontal shell-and-tube heat exchanger. Shell and tube system temperature gradients were evaluated and compared. Results showed axial and radial phase change enhancements of 2.5 and 3.5%. Esapour et al. [14] quantitatively studied the influence of inner tubes (multiple) on melting in a multi-tube heat exchanger. Single-tube splitting reduces PCM melting time by 29%. Liu et al. [15] quantitatively examined the melting process of RT27 (paraffin mix) as a PCM by employing several combinations of big and small HTF tubes. The effects of multiple-tube numbers and diameter ratios on heat transport were also examined. Combining a big and two tiny tubes with a 2:1 diameter ratio accelerated PCM melting. Liu et al. [16] performed numerical research of LTESS with staggered and parallel HTF tubes utilizing paraffin as PCM and air as HTF. Staggered tubes boost convective heat transmission and melting rate by 57%. Jesumathy et al. [17] investigated the effects of HTF temperature and mass flow rates on paraffin wax melting in a horizontal double-pipe heat storage system. A 2C change in HTF intake temperature increased melting by 25%. Kousha et al. [18] studied melting and solidification of finless multi-tube heat exchangers at various HTF temperatures. PCM was paraffin (RT-35) kept in cylinders. Four HTF tubes lowered melting and solidification times by 43% and 50%, respectively. Joybari et al. [19] examined paraffin (RT-60) melting in finless single and multiple (five) tubes vertical heat exchangers. Multi-tube arrangement increased convective effects and hastened PCM melting. Multi-tube arrangement decreased melting time by 73.6%. Although multi-tube LTESS tests have been done, most lack fins. Fins and multi-tube HTF arrangements may speed the melting process. Longitudinal fins, circular fins, and pin fins increase LTESS performance [19-23]. Yousef et al. [24] employed hollow pin-type fins in a PCM-based solar still to improve heat transmission. PCM-based, traditional, and PCM-based pin finned systems were compared. Longitudinal fins charge and discharge PCMs better than circular fins [25, 26]. Different PCM melting investigations evaluated longitudinal fins [27], fin positions [28], and shell geometry [29]. Thicker, longer, and more fins decreased PCM melting time. Yang et al. [30] studied PCM paraffin RT35 melting in an annularly finned horizontal LTESS. Installing varied numbers of annular fins around HTF tube examined PCM melting. Optimal annularly finned LTESS with 31 fins reduced melting time by 65%. Wang et al. [31] analyzed the influence of thermo-physical and geometrical factors on sleeve-tube horizontal LTESS performance. For PCM melting, fin length, geometry, angle between fins, and conductive shells were studied. Finned LTESS with fin angles of 600 and 900 decreased PCM melting time by 49.1%.

The outcomes of this study provide novel approaches for evaluating the thermal stability of PCMs (Paraffines and Lauric acid). The using of PCM in triplex heat exchanger (every side has different PCM type) enhances thermal control and stability, and provides effective thermal storage possibility. The using of different type of PCMs provides the cost effective thermal storage system by using expensive PCMs at minimum quantity. The numerous different types of fins that are being used in this study are something that has not been mentioned in any of the previous investigations. The statistical program that was utilized in the numerical investigation was properly set, which made it possible to achieve a complex statistical configuration. A numerical research has been incorporated as a component of this thesis to increase the numerical section in order to validate the outcomes of the experimental work that was done on this complex system.

2. METHODOLOGY

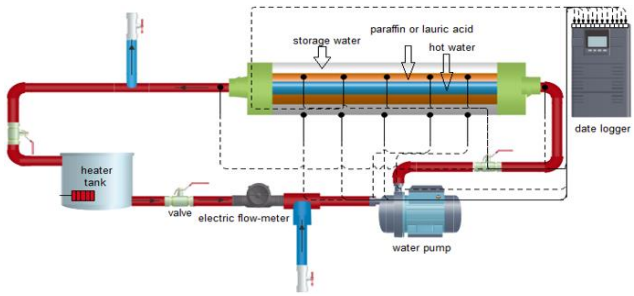

Figure 1a. Experimental process of present work

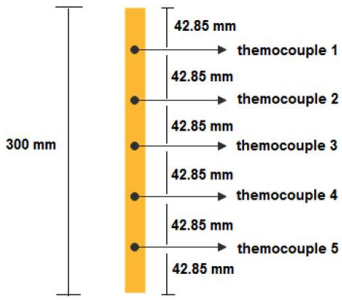

Figure 1b. Thermocouples positions

The experimental work contains the study of PCM behavior in triple pipe type heat exchanger are used. The aim of the experimental study is to find the effect of flow rates, heat transfer processes (heating and cooling), PCM type, and experimental configuration on heat storage efficiency%. The accurate measurement devices were used to collect the data and the high quality statistical approach is used to find the empirical correlation for the present work. In this chapter, the experimental procedure, the data- collection, data- analysis, and statistical approach are discussed briefly. The present system rig setup is mentioned in Figure 1a which consists of the following elements:

1. Triple pipe heat exchanger consists of three pipes, inner for water flow, intermediate which used to place PCM1 and the outer for PCM2 placement.
2. Water storage tank
3. Water pump
4. Flow meter
5. Valves
6. Insulation
7. Data logger
8. Measuring instruments and sensors
9. Heater

At various locations in the experimental apparatus, the temperature is measured using K-type thermocouples, model number TP-01K. The positions of thermocouples are mentioned in Figure 1b.

For each experiment, the heat exchanger is loaded with paraffin wax (interior tube), lauric acid (exterior tube), and water flew inside the inner tube (inside the interior tube). The

experiment used water flow rates of (11, 25, 38, and 52 L/min), flow rates are adjustable using an electronic valve. To study the smelting process of each combination, the pump was turned on. After adjusting the water flow rate to the desired value, the operation continued until both PCMs melted, then the hot side pump was turned off. To study the solidification process of each group, the cold pump was turned on after the water flow rate was set to the same value as in the previous operation. The cold pump was turned off after both PCMs solidified completely. The data logger records the information when the device is being charged and discharged. Operation of the PCM- heat exchanger for both hot and cold water flow rates, inlet and exit water temperatures, and distribution of internal temperature.

Numerically modeling the triple heat exchanger of the thermal storage tank is accomplished with the help of COMSOL Multiphysics 5.6. In Table 1, all of the pertinent physical attributes are included. At various stages of the melting process, the steady-state streamlines and transient thermal profile, as well as the melting zones, were provided by the coupled heat transfer and momentum transport equations, which were used to describe the melting process for several PCMs. These equations provided the information necessary to determine the melting zones. The following are the key transport equations that will be used throughout this paper [32, 33]:

●Continuity equation

$$\frac{1}{r}\frac{\partial}{\partial r}(ru_r)+\frac{1}{r}\frac{\partial}{\partial \theta}(u_\theta)+\frac{\partial U_z}{\partial z}=0 \tag{1}$$

●Momentum equation

$$\rho\left(U_r\frac{\partial}{\partial r}(u_r)+\frac{u_\theta}{r}\frac{\partial}{\partial \theta}(u_r)+u_z\frac{\partial U_r}{\partial z}\right) = -\frac{dp}{dr}+F_r+\mu\left(\frac{1}{r}\frac{\partial u_r}{\partial r}+\frac{1}{r^2}\frac{\partial^2 u_r}{\partial \theta^2}+\frac{\partial^2 u_r}{\partial z^2}\right) \tag{2a}$$

$$\rho\left(U_r\frac{\partial}{\partial r}(u_\theta)+\frac{u_\theta}{r}\frac{\partial}{\partial \theta}(u_\theta)+u_z\frac{\partial u_\theta}{\partial z}\right) = -\frac{dp}{d\theta}+F_\theta+\mu\left(\frac{1}{r}\frac{\partial u_\theta}{\partial r}+\frac{1}{r^2}\frac{\partial^2 Uu_\theta}{\partial \theta^2}+\frac{\partial^2 u_\theta}{\partial z^2}\right) \tag{2b}$$

$$\rho\left(U_r\frac{\partial}{\partial r}(u_{\theta z})+\frac{u_\theta}{r}\frac{\partial}{\partial \theta}(u_z)+u_z\frac{\partial u_z}{\partial z}\right) = -\frac{dp}{dz}+F_z+\mu\left(\frac{1}{r}\frac{\partial u_z}{\partial r}+\frac{1}{r^2}\frac{\partial^2 Uu_z}{\partial \theta^2}+\frac{\partial^2 u_z}{\partial z^2}\right) \tag{2c}$$

●Energy equation

$$\rho\left(U_r\frac{\partial T}{\partial r}+\frac{u_\theta}{r}\frac{\partial T}{\partial \theta}+u_z\frac{\partial T}{\partial z}\right) = Q+K\left(\frac{1}{r}\frac{\partial T}{\partial r}+\frac{1}{r^2}\frac{\partial^2 T}{\partial \theta^2}+\frac{\partial^2 T}{\partial z^2}\right) \tag{3}$$

The PCMs viscosity can be calculated from the following model [17]:

$$\mu = 0.001\exp\left(-4.25+\frac{1790}{T}\right) \tag{4}$$

The resultant density and heat capacity of PCMs composites can be calculated by using mixing rules. The melting fraction can be defined as the ratio of the latent heat to the total enthalpy, which was derived in the previous work investigation [17] and expressed as follows:

$$melting\ fraction = \frac{T-T_s}{T_l-T_s} \tag{5}$$

The geometry of the numerical solution and mesh distribution can be seen in Figure 1. The boundary conditions are mentioned in Table 2.

The main assumptions are taken into consideration:

-Steady state models.

-The geometry coordinate is three dimensions with constant surface area and symmetric with finite slides with perpendicular direction.

-The boundary walls are non- slip conditions.

-The fluid flow is laminar.

Table 1. Physical properties of PCMs [13]

PCMs	ρ, Kg/m^3	K, W/m^2.K	Cp, J/Kg.K	Melting Point (°C)
Paraffin	850	0.4	2200	52
Lauric acid	800	0.3	2500	44

Table 2. Boundary conditions of thermal storage system

Boundary conditions	value
Inlet flow rates	11-52 LPM
Outlet pressure	0 pa
Initial temperature	293 K
Inlet temperature	75°C then 27°C

Figure 2 shows that in addition to the pressure, the reference temperature of 293 degrees Celsius is also employed in order to construct the density distribution that is present inside of the heat exchanger C. The temperature used as a reference is what is used to calculate the fluid flow physical characteristics (viscosity and pressure). First, the fluid flow equation, also known as the momentum transfer equation, which is based on the Navier-Stokes mean is solved, and then, after that, the velocity profile is generated.

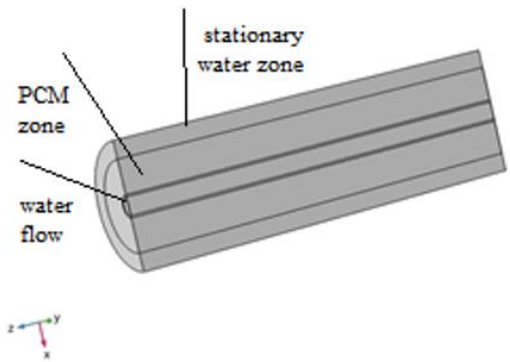

(a)

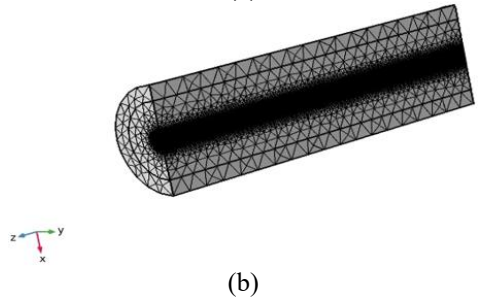

(b)

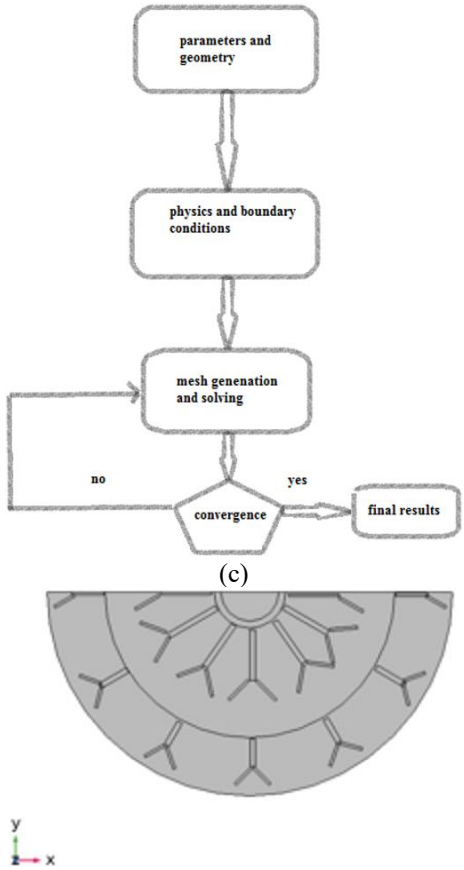

Figure 2. (a) geometry view, (b) mesh distribution, (c) CFD flow chart, (d) Finned heat exchanger

First, the reference temperature is used to produce the thermal physical attributes (thermal conductivity and heat capacity); second, the heat transfer equation is solved with the assistance of the momentum transport equation; and third, the temperature distribution is gradually prevailed over until it is reached the desired state. Beginning with the first phase, in which the new temperature distribution is utilized in place of the reference temperature, and going forward, the trial and error procedure is iterated numerous times. The increased temperature will cause changes to the distribution of physical characteristics and velocity, and the cycle will continue to be iterated step by step until the error rate in the residence time is closer to 0.1 percent or less. These changes will occur because of the increased temperature.

The temperature along the heat exchanger is collected along operation time. The average temperature is taken to obtain the stored heat which is accumulative component.

$$q_i = m\, Cp(T_{i+1} - T_i) \tag{6}$$

and

$$used\ heat = \sum_{m=0}^{i-1} q_m = q_0 + q_1 + \cdots q_{i-1} \tag{7}$$

where, q is used heat for storage, m is PCM mass, i is current situation index.

The storage efficiency can be found:

$$heat\ storage\ eff.\% = \frac{used\ heat}{latent\ heat} * 100 \tag{8}$$

Figure 3 shows the mesh element number vs. film temperature. The various mesh grids are used (Extra coarse, coarser, coarse, normal, and fine). The optimum mesh is coarse where the fine close efficiency% is achieved with minimum solution run time. Coarse mesh is used for whole numerical investigation. The increasing of mesh elements prevail no significant changes in efficiency%.

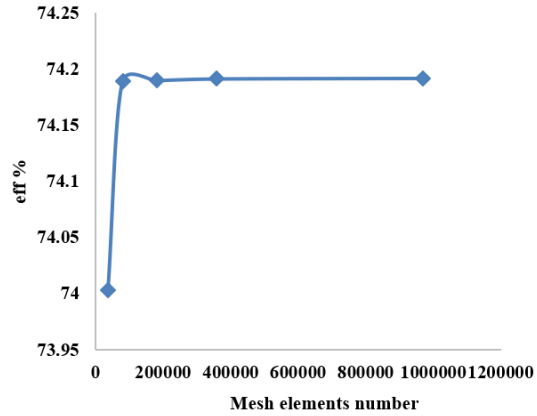

Figure 3. Efficiency percent against Mesh elements number of present investigation

3. RESULTS AND DISCUSSIONS

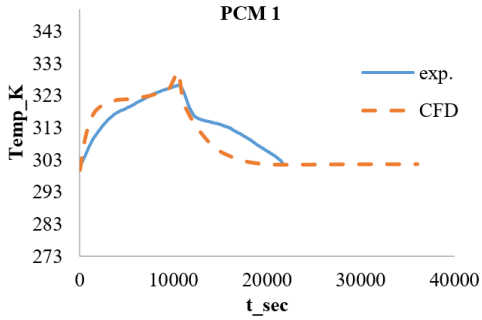

Figure 4. The validation analysis, F=52 L/min: Paraffin

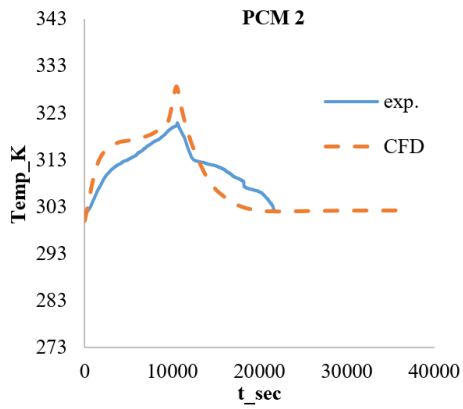

Figure 5. The validation analysis, F=52 L/min: Lauric acid

The physical parameters of different PCMs are adjusted to perform computational fluid dynamics (CFD) and heat transfer. Figures 4 and 5 show a comparison of experimental work and CFD for temperature vs. time for water at different flow rates in heat discharge and heat charge operations. The overall patterns suggest that the CFD and experimental work are in excellent accord. PCM 2 has a greater validity than paraffin.

The validity diminishes as the flow rate increases; the highest validation is seen at 11 L/min. The highest validation percentage is observed in the heat charge procedure, LAURIC ACID at 11L/MIN approximate values of 97%. The minimal validation percentage in the heat discharge process employing LAURIC ACID at a flow rate of 52 L/min is 90%. The overall tendency indicates that raising the flow rate reduces the validation percentage. LAURIC ACID has more validation than paraffin. The validity percentage of the heat discharge process is lower than the validation% of the heat charge process. The used fins have size of 11 mm length and pair of branched fins of 6 mm. the thickness of 0.6 mm is used as mention in Figure 2(d). The fins are placed on the surface of inner tube and intermediate tube in same direction. The sizes of inner tube fins are not affected by inner tube size where the 12 fins are used.

Figures 6a and 7a compare the efficiency% vs. period time plots for different operation procedures and flow rates for lauric acid in fins and without fins scenarios. The decreased flow rate encourages a 15% increase in efficiency, with a maximum efficiency of 39%. (Lower than paraffin). The paraffin functions as a resistance layer, and the conductive heat transfer in lauric acid is lower than in paraffin due to the thermal storage effect of paraffin, which absorbs a greater quantity of heat, increasing the rate of heat transfer to paraffin.

Figures 6b and 7b compare the melting fraction vs. period time plots for different operation procedures and flow rates for lauric acid in fins and without fins scenarios. The presence of fins enhances the liquid fraction in present system in both flow rates. The higher flow rate (52 LPM) depicts the faster phase transition in lauric acid especially in without fins case. The fins presence promotes the heat transfer into PCMs making the efficient phase change action.

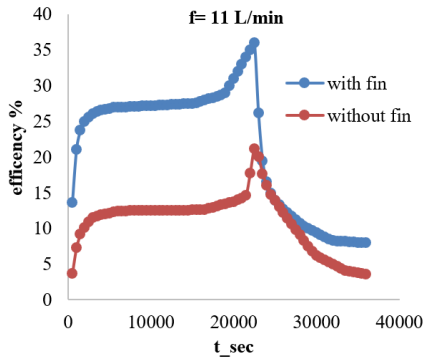

Figure 6a. Time dependent efficiency of the cases of fins presence and without fins case at F=11 L/ min and lauric acid

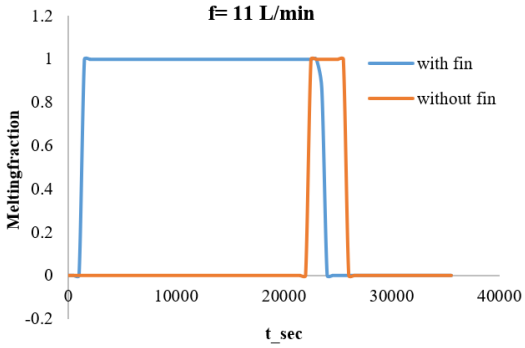

Figure 6b. Time dependent melting fraction of the cases of fins presence and without fins case at F=11 L/ min and lauric acid

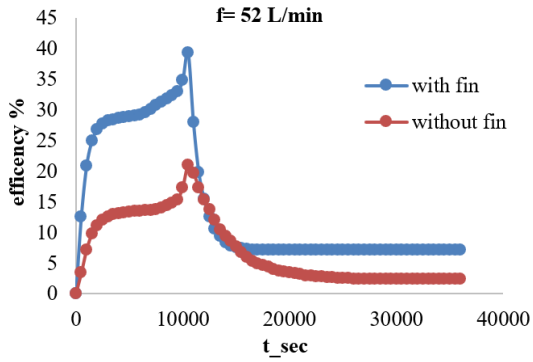

Figure 7a. Time dependent efficiency of the cases of fins presence and without fins case at F=52 L/ min and lauric acid

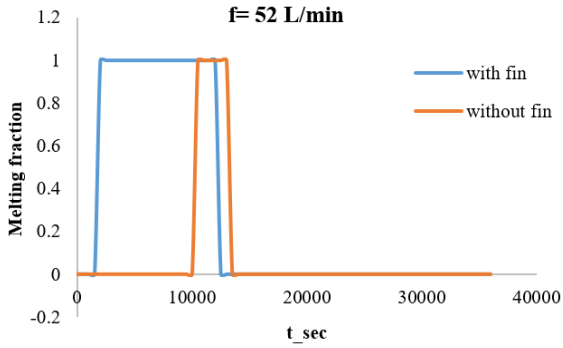

Figure 7b. Time dependent Melting fraction of the cases of fins presence and without fins case at F=52 L/ min and lauric acid

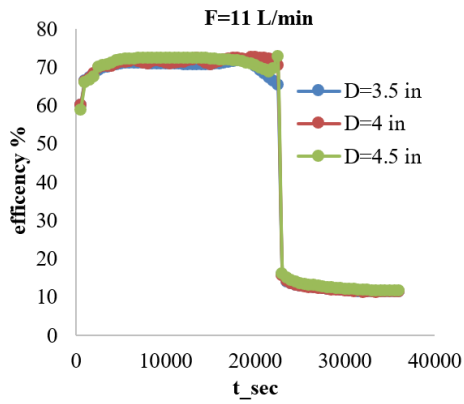

Figure 8. Time dependent efficiency for various outlet pipe diameter at F=11 L/ min and paraffin

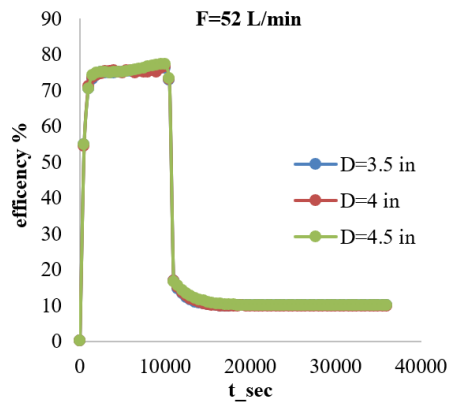

Figure 9. Time dependent efficiency for various outlet pipe diameter at F=52 L/ min and paraffin

Figures 8 and 9 demonstrate the effect of outer pipe diameter on efficiency% for different paraffin flow rates. The diameter of the pipe has no influence on the paraffin efficiency percentage. The wider the diameter of the lauric acid layer, the greater the heat resistance with a consistent heat transfer area between the paraffin and lauric acid layers. Figures 10 and 11 depict the effect of outer pipe diameter on efficiency% for different lauric acid flow rates. In the heat charge process, increasing the outside diameter results in an increase in efficiency. The highest efficiency% is found at 4.5 in. More lauric acid is produced at the largest outer diameter with finer intermediate; more lauric acid absorbs heat from paraffin. Higher flow rate (52 L/min) results in a 5% increase in efficiency. The heat discharge method has no discernible impact.

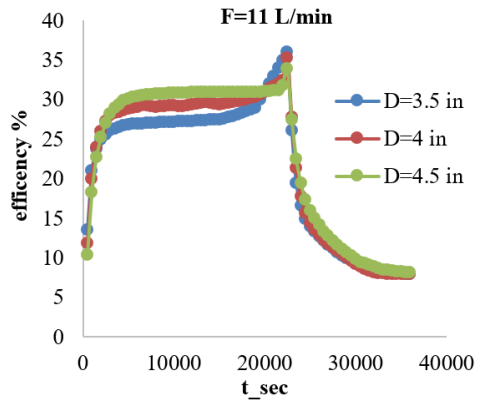

Figure 10. Time dependent efficiency for various outlet pipe diameter at F=11 L/ min and lauric acid

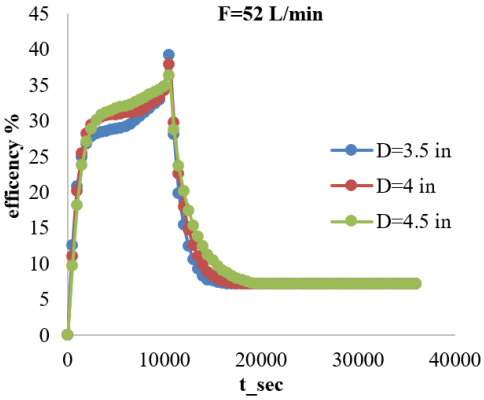

Figure 11. Time dependent efficiency for various outlet pipe diameter at F=52 L/ min and lauric acid

Figure 12 depicts the temperature distribution across several time periods and two flow rates (11 and 52 L/min). Heat transmission occurs substantially faster at greater flow rates, with temperature saturation occurring sooner than at lower flow rates. The red zone diffuses at a rate of 52 L/min rather than 11 L/min. Temperature diffusion through the paraffin area increases significantly as the inner diameters increase. The minimalizing the quantity of used paraffin by inner diameters increasing helps the thermal saturation to be accelerated. The paraffin's thermal conductivity in cooling discharge is less than heat charge, so no significant changes with inner pipe diameter would happen [32].

The validation study used the same starting and boundary circumstances, as well as thermo-physical characteristics, as the reference experiments. First, Mahdi et al. [32] reported experimental data on paraffin (RT82) melting in a longitudinally-finned triplex-tube heat exchanger, which was utilized to validate the conclusions of this study. Figure 13 depicts a comparison of the average PCM temperature throughout time. With Mahdi et al. [32], the current study has great validation.

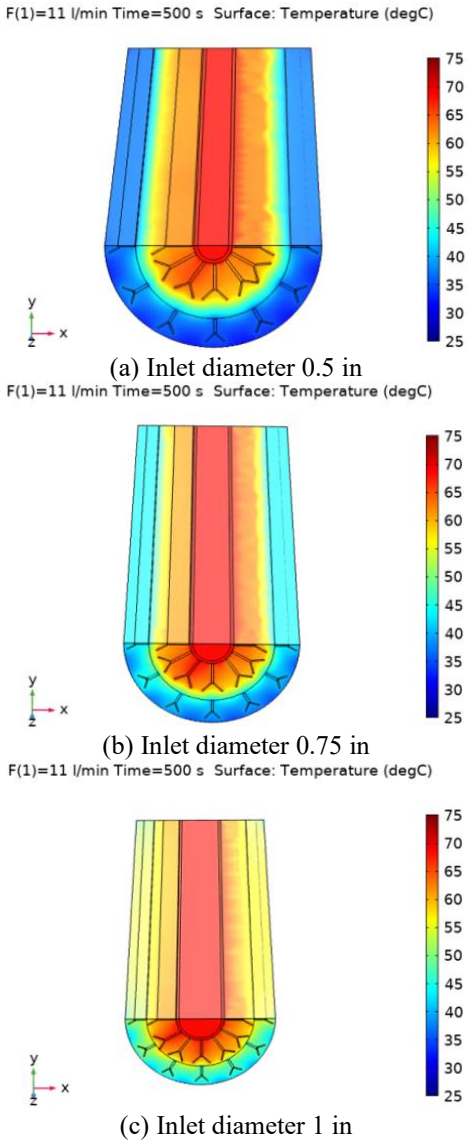

(a) Inlet diameter 0.5 in

(b) Inlet diameter 0.75 in

(c) Inlet diameter 1 in

Figure 12. Temperature distribution for various inner diameter

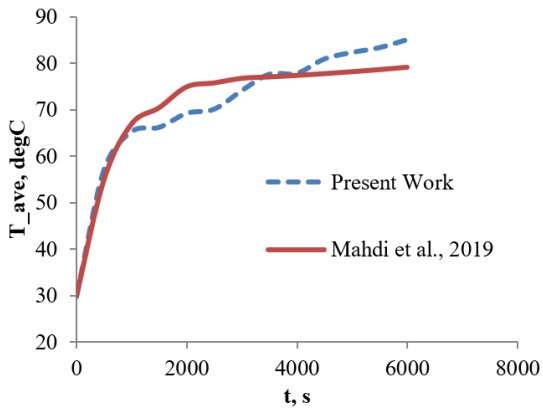

Figure 13. The comparison between present work and Mahdi et al. [32]

4. CONCLUSIONS

CFD and experimental work agree generally. PCM 2 is better than paraffin. Highest validity at 11 L/min. Fins boost efficiency by 5% (from 6 to 4); fins exceeding 6 have little effect. Extra fins may boost heat transmission by reducing heat transfer resistance. PCM and flow rates show no substantial influence of fins materials on efficiency%, especially at 11 and 52 L/min. Copper fins boost lauric acid by 2%. Copper conducts heat better than iron and aluminum. Aluminum's efficiency is equivalent to copper's, and its price is lower. Pipe diameter doesn't affect paraffin efficiency. With a uniform heat transfer area between the paraffin and lauric acid layers, the larger the lauric acid layer, the stronger the heat resistance. Increasing the heat charge outer diameter increases efficiency. Most efficient at 4.5 in. Lauric acid absorbs greater heat from paraffin at the highest outer diameter with finer intermediate. 52 L/min boosts efficiency by 5%. Heat discharge is ineffective. Increasing inner diameter with constant intermediate diameter decreases efficiency by 7%. As inner diameter increases, less paraffin is used, reducing heat absorption. At fixed intermediate diameter, increasing inner diameter improves efficiency by up to 10%. Less paraffin would reduce heat absorption, enabling lauric acid to absorb more heat. The validation research employed the identical beginning and boundary conditions as the reference experiments. First, Mahdi et al. [32] provided experimental results on paraffin (RT82) melting in a longitudinally-finned triplex-tube heat exchanger.

REFERENCES

[1] Wen, R., Zhang, W., Lv, Z., Huang, Z., Gao, W. (2018). A novel composite Phase change material of Stearic Acid/Carbonized sunflower straw for thermal energy storage. Materials Letters, 215: 42-45. https://doi.org/10.1016/j.matlet.2017.12.008

[2] Papadimitratos, A., Sobhansarbandi, S., Pozdin, V., Zakhidov, A., Hassanipour, F. (2016). Evacuated tube solar collectors integrated with phase change materials. Solar Energy, 129: 10-19. https://doi.org/10.1016/j.solener.2015.12.040

[3] Muratore, C., Aouadi, S.M., Voevodin, A.A. (2012). Embedded phase change material microinclusions for thermal control of surfaces. Surface and Coatings Technology, 206(23): 4828-4832. https://doi.org/10.1016/j.surfcoat.2012.05.030

[4] Du, K., Calautit, J., Wang, Z., Wu, Y., Liu, H. (2018). A review of the applications of phase change materials in cooling, heating and power generation in different temperature ranges. Applied energy, 220: 242-273. https://doi.org/10.1016/j.apenergy.2018.03.005

[5] Liu, C., Groulx, D. (2014). Experimental study of the phase change heat transfer inside a horizontal cylindrical latent heat energy storage system. International Journal of Thermal Sciences, 82: 100-110. https://doi.org/10.1016/j.ijthermalsci.2014.03.014

[6] Zhang, N., Yuan, Y., Cao, X., Du, Y., Zhang, Z., Gui, Y. (2018). Latent heat thermal energy storage systems with solid–liquid phase change materials: a review. Advanced Engineering Materials, 20(6): 1700753. https://doi.org/10.1002/a-dem.201700753

[7] Liu, C., Yuan, Y., Zhang, N., Cao, X., Yang, X. (2014). A novel PCM of lauric–myristic–stearic acid/expanded graphite composite for thermal energy storage. Materials Letters, 120: 43-46. https://doi.org/10.1016/j.matlet.2014.01.051

[8] Cabeza, L.F., Castell, A., Barreneche, C.D., De Gracia, A., Fernández, A.I. (2011). Materials used as PCM in thermal energy storage in buildings: A review. Renewable and Sustainable Energy Reviews, 15(3): 1675-1695. https://doi.org/10.1016/j.rser.2010.11.018

[9] Regin, A.F., Solanki, S.C., Saini, J.S. (2008). Heat transfer characteristics of thermal energy storage system using PCM capsules: a review. Renewable and Sustainable Energy Reviews, 12(9): 2438-2458. https://doi.org/10.1016/j.rser.2007.06.009

[10] Sarı, A., Karaipekli, A. (2007). Thermal conductivity and latent heat thermal energy storage characteristics of paraffin/expanded graphite composite as phase change material. Applied thermal engineering, 27(8-9): 1271-1277. https://doi.org/10.1016/j.applthermaleng.2006.11.004

[11] Akgün, M., Aydın, O., Kaygusuz, K. (2008). Thermal energy storage performance of paraffin in a novel tube-in-shell system. Applied thermal engineering, 28(5-6): 405-413. https://doi.org/10.1016/j.applthermaleng. 2007.05.013

[12] Yuan, Y., Zhang, N., Tao, W., Cao, X., He, Y. (2014). Fatty acids as phase change materials: A review. Renewable and Sustainable Energy Reviews, 29: 482-498. https://doi.org/10.1016/j. rser.2013.08.107

[13] Agyenim, F., Eames, P., Smyth, M. (2010). Heat transfer enhancement in medium temperature thermal energy storage system using a multitube heat transfer array. Renewable Energy, 35(1): 198-207. https://doi.org/10.1016/j.renene.2009.03.0 10

[14] Esapour, M., Hosseini, M.J., Ranjbar, A.A., Pahamli, Y., Bahrampoury, R. (2016). Phase change in multi-tube heat exchangers. Renewable Energy, 85: 1017-1025. https://doi.org/10.1016/j.renene.2015.07.063

[15] Liu, H., Li, S., Chen, Y., Sun, Z. (2014). The melting of phase change material in a cylinder shell with hierarchical heat sink array. Applied thermal engineering, 73(1): 975-983. https://doi.org/10.1016/j.applthermaleng.2014.08.062

[16] Liu, J., Xu, C., Ju, X., Yang, B., Ren, Y., Du, X. (2017). Numerical investigation on the heat transfer enhancement of a latent heat thermal energy storage system with bundled tube structures. Applied Thermal Engineering, 112: 820-831. https://doi.org/10.1016/j.applthermaleng.2016.10.144

[17] Jesumathy, S.P., Udayakumar, M., Suresh, S., Jegadheeswaran, S. (2014). An experimental study on heat transfer characteristics of paraffin wax in horizontal double pipe heat latent heat storage unit. Journal of the Taiwan Institute of Chemical Engineers, 45(4): 1298-1306. https://doi.org/10.1016/j.jtice.2014.03.007

[18] Kousha, N., Rahimi, M., Pakrouh, R., Bahrampoury, R. (2019). Experimental investigation of phase change in a multitube heat exchanger. Journal of Energy Storage, 23: 292-304. https://doi.org/10.1016/j.est.2019.03.024

[19] Joybari, M.M., Seddegh, S., Wang, X., Haghighat, F. (2019). Experimental investigation of multiple tube heat transfer enhancement in a vertical cylindrical latent heat thermal energy storage system. Renewable Energy, 140: 234-244. https://doi.org/10.1016/j.renene.2019.03.037

[20] Alizadeh, M., Pahlavanian, M.H., Tohidi, M., Ganji, D. D. (2020). Solidification expedition of Phase Change Material in a triplex-tube storage unit via novel fins and SWCNT nanoparticles. Journal of Energy Storage, 28: 101188. https://doi.org/10.1016/j.est.2019.101188

[21] Yuan, Y., Cao, X., Xiang, B., Du, Y. (2016). Effect of installation angle of fins on melting characteristics of annular unit for latent heat thermal energy storage. Solar Energy, 136: 365-378. https://doi.org/10.1016/j.solener.2016.07.014

[22] Mosaffa, A.H., Talati, F., Tabrizi, H.B., Rosen, M.A. (2012). Analytical modeling of PCM solidification in a shell and tube finned thermal storage for air conditioning systems. Energy and buildings, 49: 356-361. https://doi.org/10.1016/j.enbuild.2012.02.053

[23] Baby, R., Balaji, C. (2013). Thermal optimization of PCM based pin fin heat sinks: an experimental study. Applied Thermal Engineering, 54(1): 65-77. https://doi.org/10.1016/j.applthermaleng.2012.10.056

[24] Yousef, M.S., Hassan, H., Kodama, S., Sekiguchi, H. (2019). An experimental study on the performance of single slope solar still integrated with a PCM-based pin-finned heat sink. Energy Procedia, 156: 100-104. https://doi.org/10.1016/j.egypro.2018.11.102

[25] Sun, Z., Fan, R., Yan, F., Zhou, T., Zheng, N. (2019). Thermal management of the lithium-ion battery by the composite PCM-Fin structures. International Journal of Heat and Mass Transfer, 145: 118739. https://doi.org/10.1016/j.ijheatmasstransfer.2019.118739

[26] Acır, A., Canlı, M.E. (2018). Investigation of fin application effects on melting time in a latent thermal energy storage system with phase change material (PCM). Applied Thermal Engineering, 144: 1071-1080. https://doi.org/10.1016/j.applth ermaleng.2018.09.013

[27] Sciacovelli, A., Gagliardi, F., Verda, V. (2015). Maximization of performance of a PCM latent heat storage system with innovative fins. Applied Energy, 137: 707-715. https://doi.org/10.1016/j.apenergy.2014.07.015

[28] Mat, S., Al-Abidi, A.A., Sopian, K., Sulaiman, M.Y., Mohammad, A.T. (2013). Enhance heat transfer for PCM melting in triplex tube with internal-external fins. Energy Conversion and Management, 74: 223-236. https://doi.org/10.1016/j.enconm an.2013.05.003

[29] Khan, Z., Khan, Z., Tabeshf, K. (2016). Parametric investigations to enhance thermal performance of paraffin through a novel geometrical configuration of shell and tube latent thermal storage system. Energy Conversion and Management, 127: 355-365. https://doi.org/10.1016/j.enconman.2016.09.030

[30] Yang, X., Lu, Z., Bai, Q., Zhang, Q., Jin, L., Yan, J. (2017). Thermal performance of a shell-and-tube latent heat thermal energy storage unit: Role of annular fins. Applied Energy, 202: 558-570. https://doi.org/10.1016/j.apenergy.2017.05.007

[31] Wang, P., Yao, H., Lan, Z., Peng, Z., Huang, Y., Ding, Y. (2016). Numerical investigation of PCM melting process in sleeve tube with internal fins. Energy Conversion and Management, 110: 428-435. https://doi.org/10.1016/j.enconman.2015.12.042

[32] Mahdi, J.M., Lohrasbi, S., Ganji, D.D., Nsofor, E.C. (2019). Simultaneous energy storage and recovery in the triplex-tube heat exchanger with PCM, copper fins and Al_2O_3 nanoparticles. Energy Conversion and Management, 180: 949-961. https://doi.org/10.1016/j.enconman.2018.11.038

NOMENCLATURE

Symbol	Meaning	Unit
P	pressure	Kpa
A	surface area	m^2
h	heat transfer coefficient	$W/m^2.K$
T	temperature	K
Cp	heat capacity	J/kg.K
k	thermal conductivity	W/m.K
ρ	density	kg/m^3
μ	viscosity	pa.s
U	velocity	m/s
g	gravity acceleration	m/s^2